

Geochronology (Re–Os and U–Pb) and fluid inclusion studies of molybdenite mineralisation associated with the Shap, Skiddaw and Weardale granites, UK

D. Selby¹, J. Conliffe², Q. G. Crowley³ and M. Feely²

Late Devonian magmatism in Northern England records key events associated with the Acadian phase of the Caledonian–Appalachian Orogen (C–AO). Zircon U–Pb and molybdenite Re–Os geochronology date emplacement and mineralisation in the Shap (405.2 ± 1.8 Ma), Skiddaw (398.8 ± 0.4 and 392.3 ± 2.8 Ma) and Weardale granites (398.3 ± 1.6 Ma). For the Shap granite, mineralisation and magmatism are contemporaneous, with mineralisation being directly associated with the boiling of CO₂-rich magmatic fluids between 300 and 450°C, and 440 and 620 bars. For the Skiddaw granite, the Re–Os age suggests that sulphide mineralisation occurred post-magmatism (398.8 ± 0.4 Ma) and was associated with the boiling (275 and 400°C and at 375–475 bars) of a non-magmatic fluid, enriched in N₂, CH₄ and S, which is isotopically heavy. In contrast, the co-magmatic molybdenite mineralisation of the Weardale granite formed from non-fluid boiling at 476 to 577°C at 1–1.7 kbars. The new accurate and precise ages indicate that magmatism and Mo-mineralisation occurred during the same period across eastern Avalonia (cf. Ireland). In addition, the ages provide a timing of tectonism of the Acadian phase of the C–AO in northern England. Based on the post-tectonic metamorphic mineral growth associated with the Shap and Skiddaw granite aureoles, Acadian deformation in the northern England continued episodically (before ~405 Ma) throughout the Emsian (~398 Ma).

Keywords: Rhenium, Osmium, U–Pb geochronology, Molybdenite, Zircon, Fluid inclusions, Shap, Weardale, Skiddaw, Acadian orogeny

Introduction

Granitic plutons represent a significant component of orogenic cycles and are often associated with one of the most important types of fluid flow regime in the crust. Commonly the magmatic-hydrothermal systems are genetically related to Cu–Mo±Au mineralisation. The Caledonian–Appalachian Orogen (C–AO) is marked by a ~50 m.y. period of granite intrusions with associated molybdenite mineralisation systems. This study combines Re–Os molybdenite and U–Pb zircon geochronology with fluid inclusion studies to investigate the timing and nature of molybdenite mineralisation associated with the Shap, Skiddaw and Weardale granites from the northern England sector of the Acadian phase of the C–AO (Fig. 1). These three granites represent three of six

granite intrusions considered to be components of the Lake District batholith (Ennerdale, Eskdale, Threlkeld; Fig. 1). These intrusions reflect, in part, the evolution of the northern part of eastern Avalonia^{34–45} (and references therein) and the geochronology to be presented here can yield important information on the timing of tectonism during the Acadian phase of the C–AO in the northern England region. The results are further discussed in the context of granite-related molybdenite systems present in the western Ireland (Connemara) sector and in regard to the timing and duration of magmatism and also the tectonic setting of the C–AO.

Shap, Skiddaw and Weardale intrusions and associated mineralisation

The Shap granite

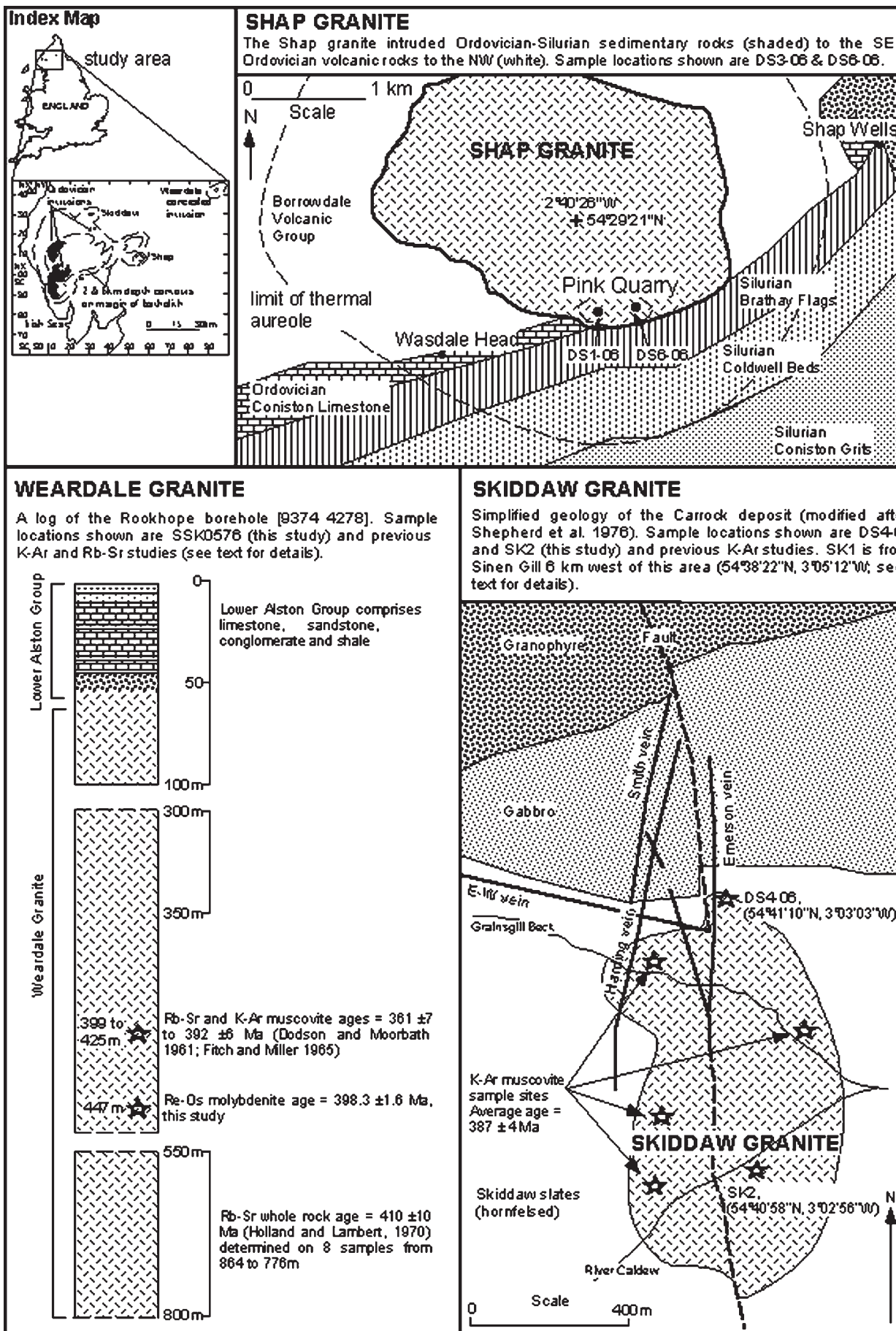
Intruded into Ordovician volcanics and Silurian sediments (Fig. 1), the Shap granite is a composite intrusion, representing three stages of magmatism. There is a progressive increase in grain size and K-feldspar megacrysts from stage one (early) to stage three (late), where the latter intrusion contains ~50 modal%

¹Department of Earth Sciences, University of Durham, Science Labs, Durham DH1 3LE, UK

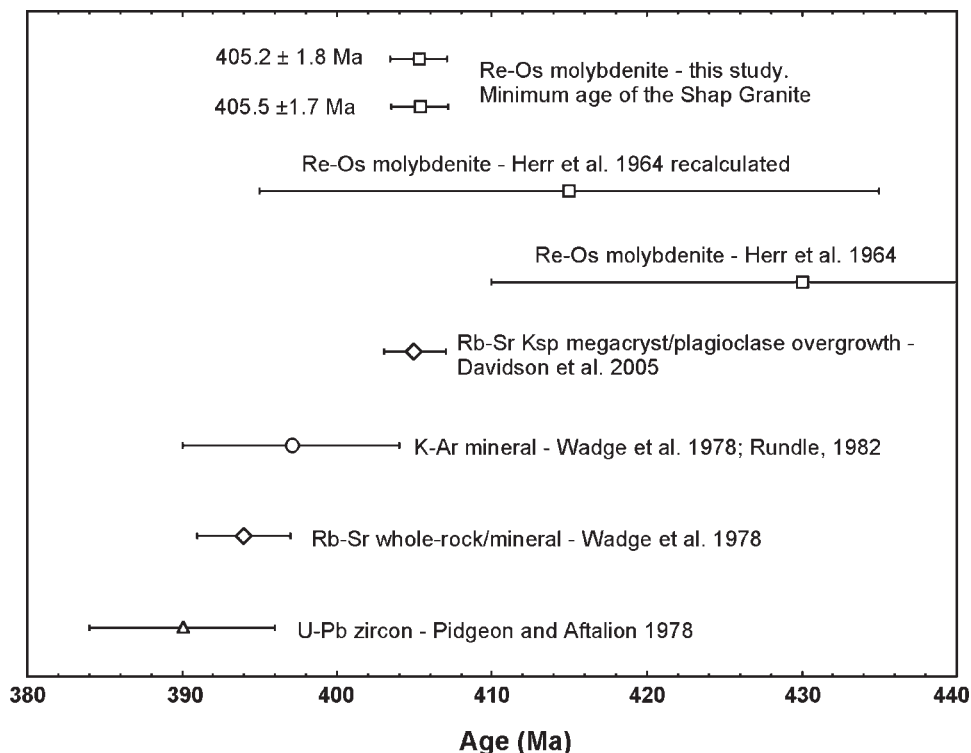
²Department of Earth and Ocean Sciences, National University of Ireland, University Road, Galway, Ireland

³NERC Isotope Geosciences Laboratory, British Geological Survey, Keyworth, Nottingham NG12 5GG, UK

Corresponding author, email david.selby@durham.ac.uk



1 Simplified geology of the studied areas, Shap granite (modified after Wadge *et al.*⁷¹), Weardale granite (modified after Dunham²⁰) and Skiddaw granite (modified after Shepherd *et al.*⁵⁹)



2 Previous age constraints for the Shap granite from U–Pb zircon, Rb–Sr whole-rock/mineral methods, K–Ar feldspar and mica, and Re–Os molybdenite geochronology: new Re–Os molybdenite ages (this study) are also shown

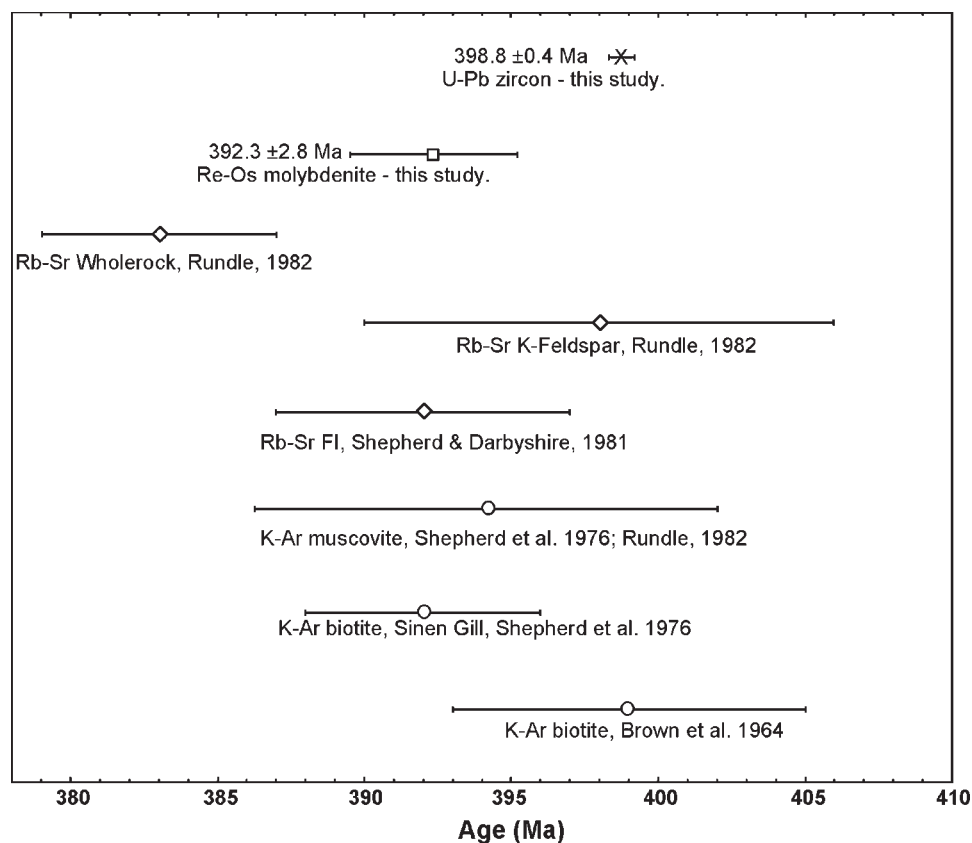
K-feldspar megacrysts.¹⁰ Stage two of the intrusion forms ~90% of the Shap granite body and comprises K-feldspar megacrysts (25–30 modal%, ~4 cm), with a matrix (1–2 mm grain size) of approximately equal amounts of quartz, orthoclase, plagioclase (oligoclase), together with lesser amounts of biotite.¹⁰ Accessory apatite, zircon, titanite are also present. All stages contain mafic enclaves. Sulphide mineralisation (pyrite–chalcopyrite–bornite ± molybdenite) in the Shap granite is both disseminated and quartz vein-hosted. Quartz veins are 1–2 cm thick, dip steeply to the east and post-date all stages of the Shap granite. The ore mineral assemblage consists of chalcopyrite–pyrite–bornite ± molybdenite. Molybdenite in some cases is the predominant ore mineral occurring with minor chalcopyrite, pyrite and bornite as both disseminations and in veins. No evidence was observed to determine the sulphide paragenesis. Quartz veins are bereft of an alteration selvage; however, matrix biotite and plagioclase are partially altered to chlorite and sericite respectively.

Several studies have presented determinations for the emplacement age of the Shap granite (Fig. 2). Uncertainties for all ages noted below are at the 2σ level. Whole-rock (stages one and two), feldspar and biotite Rb–Sr data yield an isochron age of 394 ± 3 Ma ($n=22$).⁷¹ In contrast, Rundle⁵² reported a Rb–Sr age using whole-rock data (stages two and three intrusion) of 381 ± 8 Ma. A recent single crystal Rb–Sr feldspar study yields an age of 405 ± 2 Ma.¹³ K–Ar biotite analyses from the stage two granite yields a mean age of 397 ± 7 Ma; however, individual analyses range from 394 ± 12 to 403 ± 12 Ma ($n=3$).⁷¹ A discordia of U–Pb data for three multi-grain zircon fractions yield an upper intersection age of 390 ± 6 Ma.⁵¹ Based on the agreement of this age with a mean of 21 Rb–Sr and K–Ar

ages,⁸ the U–Pb age was suggested to reflect the age of emplacement for the Shap granite. Molybdenite from the Shap granite was used in one of the first Re–Os molybdenite studies, which determined an age of 430 ± 20 Ma, using a decay constant of $1.611 \times 10^{-11} \text{ a}^{-1}$.³¹ Using the currently accepted decay constant ($1.666 \times 10^{-11} \text{ a}^{-1}$),^{57,58} an age of 415.2 ± 19 Ma is calculated. Though all the age determinations overlap within uncertainty, there is a significant degree of disparity between the nominal ages (Fig. 2).

The Skiddaw granite

The granite is genetically and spatially related to the W mineralisation of the Carrock Fell deposit. Intruded into the early Ordovician metasediments of the Skiddaw group, the Skiddaw granite outcrops are restricted to three localities (Sinen Gill, Caldew Valley and Grainsgill).⁵⁹ The latter represents the slightly smaller, though heavily mineralised and hydrothermally altered outcrop (Fig. 1). Unaltered, the Skiddaw granite is medium-grained and comprises plagioclase, orthoclase, biotite and quartz. Mineralisation is confined to the northern margin of the granite in Grainsgill and occurs in a series of steeply dipping N–S quartz veins typically ≤ 0.5 m in thickness (Harding, Smith and Emerson veins, Fig. 1).^{3,59,60} Barren early quartz veins are cross-cut by the main ore-bearing N–S trending quartz veins that carry wolframite ± scheelite.⁵⁹ Alteration associated with this mineralisation is minimal, with the exception of a greisen assemblage in the granite which also contains arsenopyrite + pyrite + apatite. Post-dating the latter is sulphide mineralisation (arsenopyrite, pyrite, chalcopyrite, molybdenite, sphalerite, bismuth) that occurs in quartz stringers in fractures of the veins and greisen zones.³ Calcite ± siderite ± fluorite veining post-dates sulphide mineralisation. Small E–W trending



3 Previous age constraints for the Skiddaw granite and the timing of mineralisation of the Carrock W tungsten deposit from K–Ar mica and Rb–Sr fluid inclusion geochronology: new Re–Os molybdenite ages (this study) are also shown

quartz–galena–sphalerite veins cross-cut the Carrock Fell mineralisation and are thought to be part of the Caldbeck Fell Pb–Zn systems to the north.

Age determinations for the Skiddaw granite and its mineralisation are restricted to K–Ar mica and Rb–Sr fluid inclusion ages (Fig. 3). Magmatic biotite from Sinen Gill yield a mean K–Ar biotite age of 399 ± 6 Ma.⁹ Overlapping within uncertainty are slightly younger K–Ar ages (392 ± 4 Ma) for magmatic biotite from Sinen Gill and Caldew Valley, which are interpreted to record the final cooling of the Skiddaw granite.⁵⁹ In accord with these ages is an Rb–Sr isochron age (398 ± 8 Ma) determined from K–Feldspar from altered granite; however, Rb–Sr whole-rock data yield a younger age of 383 ± 4 Ma.⁵² Younger ages are also reported for hydrothermal muscovite from greisen at Grainsgill and of the Harding vein (mean age of 387 ± 4 Ma),⁵² which overlaps, within uncertainty, with a Rb–Sr fluid inclusion age (392 ± 5 Ma) obtained from both early and late phases of quartz veining.⁶²

The Weardale granite

This granite is a concealed body beneath the Carboniferous rocks. It is intersected at 390.5 m below the surface in the Rookhope borehole. The boundary between the Weardale granite and Carboniferous sediments is marked by a soil-like quartz–mica-rich mudstone, which is suggested to represent the weathered surface of the granite²⁰ (and references therein). The Carboniferous sediments are not metamorphosed, suggesting that the granite pre-dates the Carboniferous rocks. The granite is medium-grained and consists of muscovite, biotite, plagioclase, orthoclase and accessory

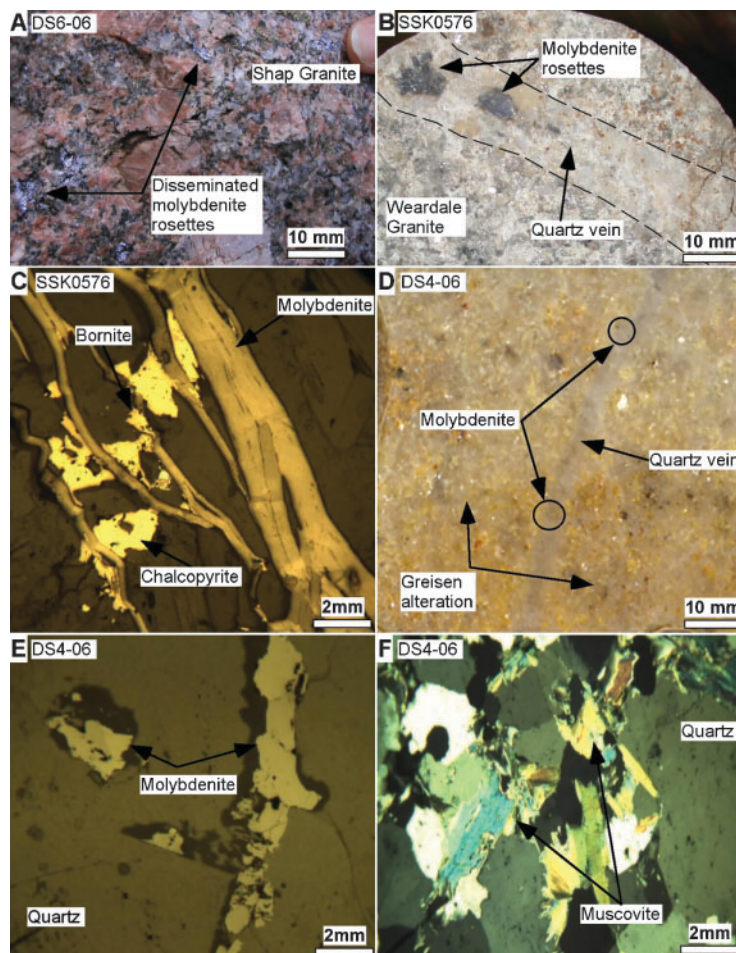
magnetite–ilmenite, zircon and monazite. Quartz and mica define a flat lying fabric, which is suggested to represent the apex of a cupola.²⁰ The granite contains veins of quartz pegmatite and aplite, a number of which are tourmaline-bearing.²⁰ At 447 m, a 3 cm wide molybdenite bearing quartz pegmatite vein cuts the granite fabric. Molybdenite mineralisation is accompanied by chalcopyrite, minor bornite and pyrite (Fig. 1). No tourmaline is observed in the quartz and the relationship between tourmaline and molybdenite mineralisation is not known. An alteration selvage is absent; however, plagioclase and biotite show minor alteration to sericite and chlorite respectively.

Early age determinations have been presented from Rb–Sr and K–Ar muscovite analyses, which range from 356 ± 12 to 392 ± 6 Ma.^{16,26} A more recent Rb–Sr whole-rock analyses from 564 to 776 m was used to suggest that the emplacement age of the Weardale granite was 410 ± 10 Ma, intrusion of post-pegmatite vein aplites at 390 ± 8 Ma, and that hydrothermal activity continued to 365 ± 8 Ma.³²

Samples and analytical protocols

Samples

Three molybdenite-bearing quartz veins were sampled from the Shap (DS1-06), Skiddaw (DS4-06) and Weardale (SSK0576) granites (Fig. 1). Suitably sized portions of each sample were used for Re–Os geochronology and fluid inclusion studies. An additional sample (DS6-06) of disseminated molybdenite from the Shap granite was also used to determine a Re–Os age. In the



4 **A** disseminated rosettes of molybdenite in the Shap granite, **B** quartz vein-bearing molybdenite rosette in the Weardale granite at 447 m in the Rookhope core, **C** photomicrograph of the quartz–molybdenite vein in the Weardale granite: minor chalcopyrite rimmed with bornite is associated with the molybdenite, **D** hand specimen from the spoil of the Emerson vein, Carrock deposit: quartz vein contains minor fine-grained molybdenite with greisen alteration, **E** photomicrograph of molybdenite in sample DS4-06, and **F** photomicrograph of the greisen alteration selvage of the quartz vein: the selvage is comprised solely of fine-grained muscovite and quartz

Shap granite, molybdenite mineralisation occurs disseminated (DS6-06) and within about 1–2 cm quartz veins (DS1-06). Molybdenite is present as ~1 cm diameter rosettes, with individual grains of a 2–5 mm (Fig. 4), and is associated with minor chalcopyrite.

In the Skiddaw granite, the molybdenite sample (DS4-06) from the Carrock deposit was taken from the surface spoil near the adit to the Emerson vein (Fig. 4). The spoil consists largely of quartz vein and greisenised Skiddaw granite (Fig. 4) and is taken to represent the mineralisation of the Emerson vein. It is a 3 mm quartz molybdenite-bearing stringer that cross-cuts a greisen altered rock and is considered to represent sulphide mineralisation that post-dates the primary W-bearing mineralisation.³ Molybdenite is fine-grained (~1 mm) and occurs as single grains throughout the stringer with minor chalcopyrite and pyrite. Minor muscovite alteration is also associated with the quartz stringer, which occurs as 1–2 mm rosettes within and on the selvages of the stringer. Because the molybdenite post-dates the main W-bearing mineralisation, two ~8 kg samples of the Skiddaw granite were taken from separate localities at Sinen Gill (SK-1) and Caldew Valley (SK-2) for U–Pb zircon geochronology (Fig. 1).

In the Weardale granite, molybdenite has only been observed at 447 m in a quartz pegmatite vein in the Rookhope core (SSK0576, Fig. 4). Molybdenite is the predominant ore mineral in this pegmatite vein occurring as ~1 cm rosettes with 2–5 mm grains, and isolated grains (Fig. 4).

Analytical protocols

The Re–Os geochronometry was performed in the Northern Centre for Isotopic and Element Tracing (NCEIT) at Durham University. Using conventional mineral separation protocols (porcelain disc milling, FRANTZ magnetic separation, heavy liquid, water flotation) molybdenite (+44–210 μm fraction) was isolated from whole-rock and quartz vein samples.⁵³

Isotope dilution, using a mixed tracer solution containing isotopically enriched ^{185}Re and isotopically normal Os, in the form of a gravimetric and isotopic Os standard, was used to determine the isotopic abundance of ^{187}Re and ^{187}Os in analysed molybdenite. Dissolution of molybdenite and equilibration of sample and tracer Re and Os was conducted in inverse *aqua regia* using the Carius-tube method. Rhenium and Os were isolated from the inverse *aqua regia* solution using solvent

extraction, micro-distillation and chromatographic techniques.⁵⁴ The purified Os and Re were loaded to Pt and Ni filaments respectively. The isotope ratios were measured using negative thermal ionization mass spectrometry on a Thermo Electron TRITON thermal ionisation mass spectrometer using Faraday collectors. Total procedural blanks during this study for Re and Os are 2 picograms (pg) and 0.5 pg respectively, with an ¹⁸⁷Os/¹⁸⁸Os blank composition of 0.17 ± 0.02 ($n=1$).

The Chinese molybdenite powder HLP-5⁶⁹ is used as an in-house and inter-laboratory 'control' (AIRIE, Colorado State University, the Radiogenic Isotope Facility, University of Alberta, NCEIT, Durham University) to assess the sample absolute age determination. For this 'control' (HLP-5), an average Re–Os age of 219.9 ± 0.7 Ma (0.32% 2σ , $n=3$) (Table 1) was determined during this study. This age is within uncertainty to that reported by Markey *et al.*⁴¹ (221.0 ± 2 Ma, 0.8% 2σ , $n=19$) and Selby and Creaser⁵³ (220.5 ± 0.2 (0.11%, $2\sigma=17$)).

Zircon fractions were analysed by isotope dilution thermal ionisation mass spectrometry (ID-TIMS) at the NERC Isotope Geosciences Laboratory (NIGL). Analytical procedures are described in Ref. 47. Zircon crystals were separated from <355 µm whole-rock fraction of SK-1 and SK-2 using standard vibrating-table, specific gravity and magnetic techniques. Crystal fractions for analysis were picked by hand under a binocular microscope. Acicular zircons, typically $150 \times 50 \times 50$ µm with visible melt inclusions, were preferentially selected in order to avoid crystals with inherited cores. A bulk zircon fraction was annealed at 850°C in quartz glass beakers for 48 h. The zircon crystals were ultrasonically washed in 4 N HNO₃, rinsed in ultra-pure water, then further washed in warm 4 N HNO₃ before rinsing with distilled water to remove surface contamination. The annealed, cleaned bulk zircon fraction was then chemically abraded in 200 µL 29 N HF and 20 µL 8 N HNO₃ at 180°C for 12 h following a modified chemical abrasion technique to remove portions of grains which have suffered Pb-loss.⁴² Chemically abraded zircons were washed several times in ultra-pure water, in warm 3 N HCl for several hours

on a hot-plate, rinsed again in ultra-pure water and 8 N HNO₃ and split into single grain fractions ready for dissolution. A mixed ²⁰⁵Pb–²³⁵U tracer was used to spike all fractions. Representative fractions were checked in cleaned PMP beakers under fibre optic light to check for complete dissolution. Dissolved, spike-equilibrated samples were not subjected to ion-exchange procedures but were converted to chloride and loaded onto degassed rhenium filaments in silica gel following a procedure modified after.⁴⁶ Isotope data were collected using a Thermo Electron Triton equipped with a new generation of MassCom secondary electron multiplier.⁴⁸ A minimum of 100 ratios were collected for Pb and 60 for U. Pb ratios were scrutinised for any evidence of organic interferences which were determined to be negligible. Uncertainties were calculated using numerical error propagation.³⁸ Isotope ratios were plotted using Isoplot version 3,³⁹ and error ellipses and ages presented reflect 2σ uncertainty. Total procedural blanks were between 0.2 and 0.6 pg for Pb and 0.1 pg for U. Samples were blank corrected for Pb, and any residual common Pb was corrected using a Stacey-Kramers common lead composition.⁶⁷

Fluid inclusion petrography and microthermometric analyses of the samples were conducted at the Geofluids Research Laboratory, NUI, Galway. Heating and freezing runs on doubly polished fluid inclusion wafers (~100 µm thick) were performed using a calibrated Linkam THMS600. Calibration with precision of $\pm 0.2^\circ\text{C}$ at -56.6°C and $\pm 1^\circ\text{C}$ at 300°C was conducted using synthetic H₂O and CO₂ standards. Following procedures outlined by Shepherd *et al.*,⁶¹ the temperature of first ice melting T_{FM} , the temperature of last ice melting T_{LM} and the temperature of homogenisation T_{H} were measured in two-phase liquid + vapour inclusions hosted in quartz in all wafers. Fluid salinities were calculated using T_{LM} and the equations of Ref. 6. In addition, clathrate melting temperatures recorded in some of these two-phase inclusions were used with the equations of Ref. 18 to calculate their fluid salinities.

Laser Raman microspectroscopy (LRM) was used to determine the non-aqueous chemical species present in fluid inclusions. Analyses were conducted at CREGU

Table 1 Re–Os isotope data for molybdenite from Shap, Weardale and Skiddaw granites

Sample	Weight, mg	¹⁸⁷ Re*, ppm	SD	¹⁸⁷ Os*, ppb	SD	Age [†]	SD
HLP-5							
1	11	174.3	±0.8	637.6	2.8	219.2	0.9
2	11	174.6	±0.8	641.4	2.9	220.0	0.9
3	10	173.5	±0.9	638.6	2.9	220.6	0.9
Weardale							
SSK0576	45	59.30	±0.19	394.8	1.0	398.3	1.6
Skiddaw							
DS4-06	70	0.47	±0.003	3.1	0.02	392.3	2.8
Shap							
DS1-06	31	9.51	±0.03	64.5	0.2	405.5	1.7
DS6-06	21	9.61	±0.06	65.1	0.2	405.2	1.8
Shap [‡]	9000	11.20	±0.40	77.8	2.3	429.3 [§]	19.9
						415.2 [¶]	19.3

All uncertainties are quoted at the 2σ level.

HLP-5 is an in-house control molybdenite powder (see text for discussion).

*Re and Os concentrations and Re–Os age recalculated using uncertainties in Re and Os mass spectrometer measurements, standard and spike Re and Os isotopic compositions, and calibration uncertainties of ¹⁸⁵Re and ¹⁸⁷Os.

[†]Age calculated using the decay constant $\lambda^{187}\text{Re} = 1.666 \times 10^{-11}/\text{year}$, without uncertainty.⁵⁸

[‡]Re–Os isotope data taken from Ref. 10.

[§]Age established using $^{187}\text{Re}\lambda = 1.612 \times 10^{-11}/\text{year}$.^{31,57,58}

[¶]Age established using $^{187}\text{Re}\lambda = 1.666 \times 10^{-11}/\text{year}$.^{31,57,58}

(Nancy, France) using a Labram (HoribaJobin) Raman microspectrometer equipped with an edge filter and a liquid nitrogen cooled charge coupled device detector. A holographic grating with 1800 grooves per millimetre was used. An exciting radiation at 514.4 nm was provided using an ionized Ar–Ar laser. The laser was focused on inclusions using an Olympus microscope with an $\times 80$ objective. The mole fraction of gaseous species was calculated using the procedure described by Ref. 19. Bulk fluid inclusion parameters and molar volumes were calculated using the LRM results in combination with the microthermometric data for each inclusion (analysed by LRM), and the computer programs CLATHRATES¹ and FLUIDS.²

Results

Re–Os molybdenite geochronology

Molybdenite from the Shap, Skiddaw and Weardale granites show considerable differences in ¹⁸⁷Re and ¹⁸⁷Os abundances (Table 1). The Weardale sample (SSK0576) has the highest ¹⁸⁷Re (59 ppm) and ¹⁸⁷Os (395 ppb) abundances, with Shap molybdenite (DS1-06, DS6-06) possessing significantly lower values of ~ 9 ppm ¹⁸⁷Re and 65 ppb ¹⁸⁷Os, and the molybdenite from the Carrock Fell deposit (Skiddaw, DS4-06) containing very low ¹⁸⁷Re (500 ppb) and ¹⁸⁷Os (3.1 ppb) contents.

The ¹⁸⁷Re and ¹⁸⁷Os systematics for all samples are used to calculate model ages with the decay constant of Ref. 58. Two molybdenite samples from Shap yield model Re–Os ages of 405.5 ± 1.7 and 405.2 ± 1.8 Ma (Table 1). The Weardale and Skiddaw molybdenite samples yield Re–Os ages of 398.3 ± 1.6 and 392.3 ± 2.8 Ma respectively (Table 1). All the Re–Os ages are outside the limits of uncertainty and therefore record distinct events in relation to the processes associated with the Shap, Weardale and Skiddaw granites.

Skiddaw granite U–Pb zircon geochronology

A total of eight single grain fractions, four from Sinen Gill and three from Caldew Valley, were utilised for U–Pb geochronology. These grains all possess high U abundances (549–4384 ppm; Table 2); seven grains overlap within error to give a concordia age of 398.8 ± 0.4 Ma (concordance and equivalence: MSWD=1.5, probability=0.11; Fig. 5), with a single grain from the Caldew Valley (SK-2) sample slightly discordant due to Pb-loss (not shown). This is taken as the emplacement age of the granite. Previous attempts at dating the Skiddaw granite from these same localities were problematic in that multi-grain fractions of zircon showed signs of inheritance (J. Evans, personal communication, 2007; unpublished BGS data). In the case of this study, single acicular grains were selected and so inheritance was avoided. Furthermore, previous attempts at dating the Skiddaw granite using the U–Pb zircon technique utilised the air-abrasion³⁵ technique to minimise the effects of Pb-loss. This would have inherently meant that delicate acicular zircons such as those used in this study would not have been previously used as they would have been destroyed by the air abrasion process. It is also noteworthy that chemical abrasion has the effect of dissolving magmatic inclusions and so reducing the common lead content.⁴²

Table 2 U–Pb zircon ID-TIMS data for the Skiddaw granite

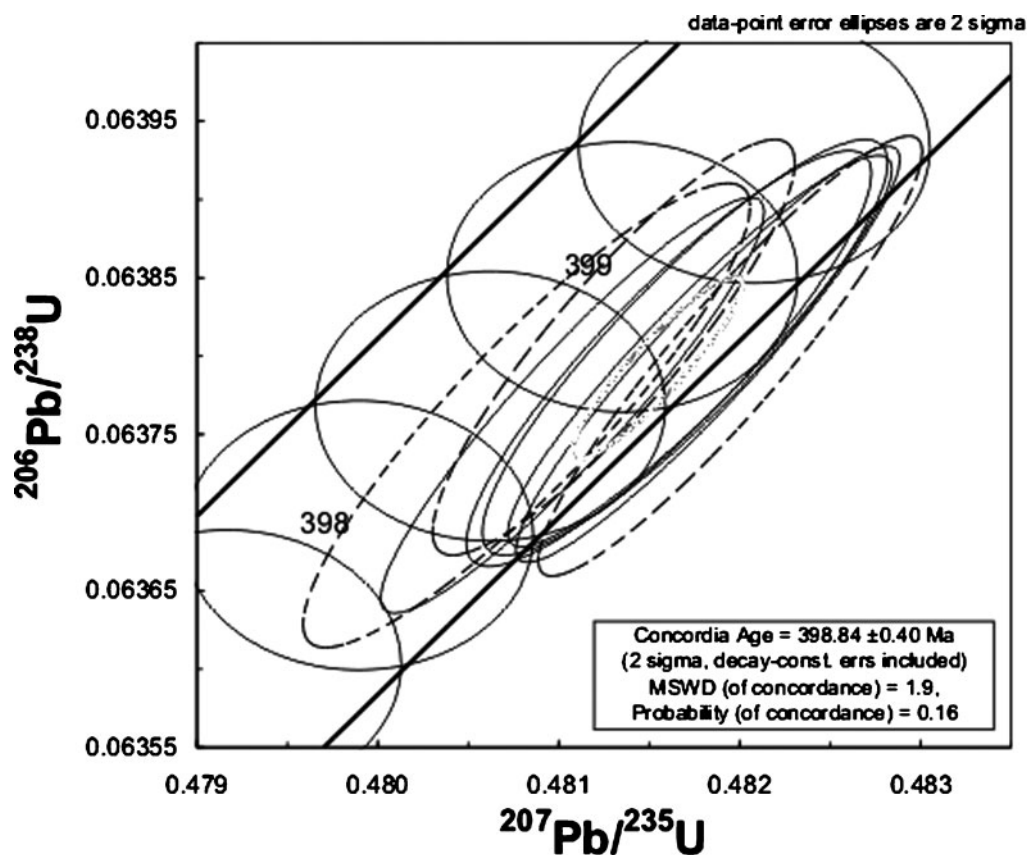
Sample	Fraction	Weight, μg	U, ppm	Cm–Pb [†] , ppm	Ratios	Ratios		Age, Ma		
						²⁰⁶ Pb/ ²⁰⁴ Pb [†]	²⁰⁷ Pb/ ²⁰⁶ Pb [†]	Rho	²⁰⁷ Pb/ ²⁰⁶ Pb	
SK-1	Z1	2.6	549	0.9	5991	0.05468	0.16	0.93	399.3	399.6
	Z2	1.2	4384	0.7	30388	0.05477	0.17	0.94	402.9	399.3
	Z3	1.3	1534	0.6	12348	0.05475	0.17	0.89	402.0	399.2
	Z4	1.0	3137	0.5	24446	0.05475	0.17	0.89	402.2	399.2
SK-2	Z5	1.3	3215	0.2	69311	0.05471	0.17	0.93	400.6	398.8
	Z1	1.0	2349	1.0	8871	0.54765	0.18	0.93	402.7	399.3
	Z3	0.8	1673	0.3	19402	0.54692	0.19	0.90	399.6	398.6
	Z5	1.0	1199	1.7	2847	0.54709	0.17	0.89	400.4	400.0

All errors are 2σ (per cent for ratios; absolute for ages).

[†]Corrected for blank Pb, U and common Pb.⁶⁷

[‡]Measured ratio, corrected for spike and Pb fractionation.

[§]Total common Pb in analysis, corrected for spike and fractionation (0.05%/amu).



5 U–Pb zircon Concordia plot for the Skiddaw granite

Fluid inclusions

The fluid inclusion petrographic study adopted the concept of fluid inclusion assemblages (FIA) described by Goldstein,²⁷ an approach that places fluid inclusions into assemblages interpreted to have been trapped at around the same time. Three types (types 1, 2 and 3) of aqueous fluid inclusion have been recognised in all three samples based on phases present at room temperature and their microthermometric behaviour (Table 3 and Fig. 6). Type 1 inclusions are vapour-rich, degree of fill F is 0.18–0.62 ($F = \text{vol. liquid}/\text{vol. liquid} + \text{vapour}$). Type 2 are liquid rich, $F = 0.47$ –0.87. The majority of types 1 and 2 fluid inclusions form trails that do not crosscut crystal boundaries and are classified here as pseudosecondary based on the criteria of McCandless *et al.*⁴⁰ In addition, a number of types 1 and 2 inclusions are hosted in clusters within the cores of quartz crystals. The authors interpret types 1 and 2 to constitute one FIA in each of the quartz vein samples from Shap and Skiddaw. In the Weardale pegmatite vein, the vapour rich type 1 inclusions are uncommon and type 2 inclusions invariably occur in annealed fractures without type 1.

The temperature of the first ice melting T_{FM} in type 1 (only recorded in the Skiddaw sample) and type 2 inclusions occurs between -19.5 and -23.7°C indicating the dominant presence of NaCl in solution. The temperature of last ice melting T_{LM} in types 1 and 2 inclusions (from -0.1 to -5.2°C) was used to calculate fluid salinities in equivalent wt-%NaCl (eq. wt-%NaCl). The range of salinities for types 1 and 2 are broadly similar, i.e. 0.2–8.1 eq. wt-%NaCl (Table 3).

In both the Shap and Skiddaw vein samples (DS1-06 and DS4-06), clathrate melting between $+5.8$ and $+10^\circ\text{C}$ was observed in some type 1 (DS1-06 only) and type 2 inclusions. This indicates the presence of non-aqueous phases in types 1 and 2 inclusions (*see the section on 'Laser Raman microspectroscopy'*), which can affect calculated fluid salinities.³⁰ Clathrate melting temperatures and bulk fluid inclusion compositions were used to calculate fluid salinities of 3.3 to 4.7 eq. wt-%NaCl, within the range calculated from T_{LM} values.

Homogenisation to the vapour phase takes place between 312.4 and 445.6°C in type 1 inclusions, whereas in type 2, homogenisation is to the liquid phase and takes place between 246 and 425°C (Fig. 7 and Table 3). On heating and before homogenisation, several types 1 and 2 inclusions in all samples decrepitated between 230.4 and 438.6°C (Table 3).

Type 3 fluid inclusions are liquid rich, $F = 0.71$ –0.99, and unlike types 1 and 2, occur along annealed fractures that cross-cut crystal boundaries and are considered to be secondary in origin. They occur in all three vein samples. Their T_{FM} values range between -19.4 and -25.2°C , thus are interpreted to reflect the dominance of NaCl in solution. T_{LM} values range from -0.2 to -4.9°C , yielding salinity values between 0.4 and 7.7 eq. wt-%NaCl (Fig. 8). Homogenisation to the liquid phase occurs between 86.6 and 296.7°C .

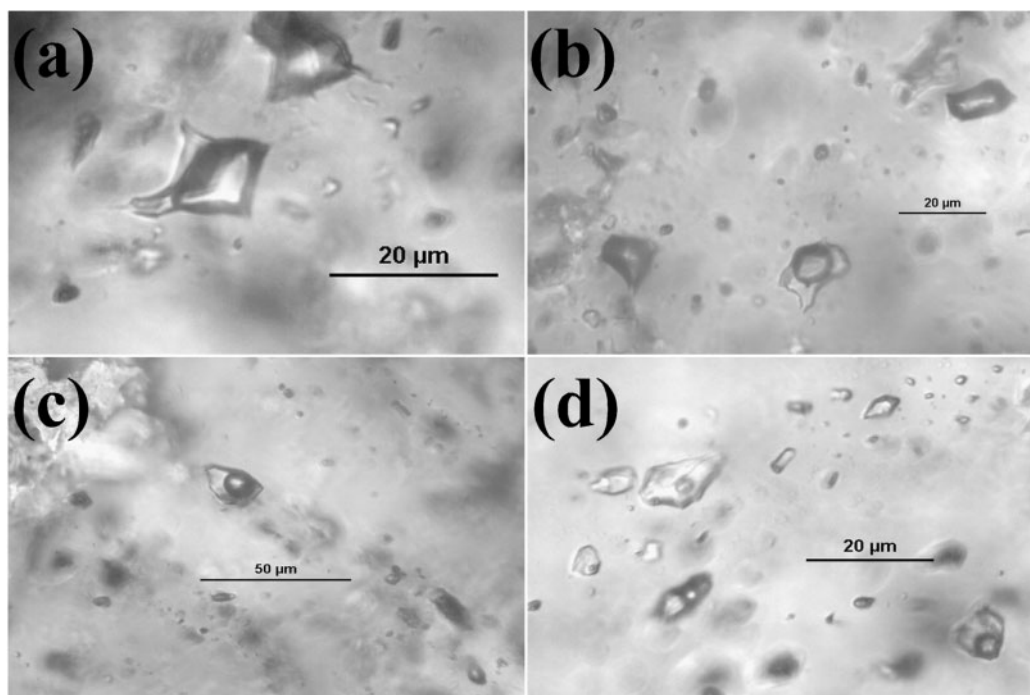
Laser Raman microspectroscopy

Laser Raman microspectroscopy (LRM) of types 1 and 2 inclusions in the three vein samples from the Shap, Skiddaw and Weardale granites revealed the presence, in

Table 3 Fluid inclusion microthermometric data from the Shap, Skiddaw and Weardale granites

Fluid inclusion type	Shap granite (DS1-06)	Skiddaw granite (DS4-06)	Weardale granite (SSK0576)
Type 1: 4–30 μm : L+V (V-rich); occur in clusters in the core of quartz crystals (unknown origin) and trails that do not crosscut crystal boundaries (pseudosecondary): ellipsoidal or irregular shapes	Abundance: 23% Fill: 0.18–0.54 (26) T_{LM} : -0.7 to -4°C (9) (1.2–6.7 eq. wt-%NaCl) $T_{\text{H}\rightarrow\text{V}}$: 357.7–448.4°C (19) T_{D} : 366.6–424.5°C (7)	Abundance: 25% Fill: 0.11–0.62 (22) T_{FM} : -20.1 to -21.6°C (2) T_{LM} : -0.4 to -2.3°C (9) (0.7–3.9 eq. wt-%NaCl) $T_{\text{H}\rightarrow\text{V}}$: 312.4–445.6°C (21) T_{D} : 408.3°C (1)	Abundance: 3% Fill: 0.43–0.61 (4) T_{LM} : -0.8°C (1) (1.4 eq. wt-%NaCl) $T_{\text{H}\rightarrow\text{V}}$: 357.7–448.4°C (3)
Type 2: 3–30 μm : L+V (L-rich); occur in clusters in the core of quartz crystals (unknown origin) and trails that do not crosscut crystal boundaries (pseudosecondary): ellipsoidal, irregular or negative crystal shapes	Abundance: 46% Fill: 0.47–0.82 (53) T_{FM} : -19.9 to -22.6°C (8) T_{LM} : -0.8 to -5°C (24) (1.4–7.9 eq. wt-%NaCl) $T_{\text{H}\rightarrow\text{L}}$: 250.7–418.9°C (29) T_{D} : 302–438.6°C (24)	Abundance: 37% Fill: 0.51–0.87 (33) T_{FM} : -19.5 to -22°C (5) T_{LM} : -0.3 to -5.2°C (17) (0.5–8.1 eq. wt-%NaCl) $T_{\text{H}\rightarrow\text{L}}$: 251.4–397.4°C (28) T_{D} : 230.4–377°C (5)	Abundance: 36% Fill: 0.4–0.86 (41) T_{FM} : -21.2 to -23.7°C (9) T_{LM} : -0.1 to -3°C (24) (0.2–5 eq. wt-%NaCl) $T_{\text{H}\rightarrow\text{L}}$: 246–425°C (30) T_{D} : 302.6–425°C (10)
Type 3: 2–25 μm : L+V (L-rich); occur in trails that crosscut crystal boundaries (secondary): ellipsoidal or irregular shapes	Abundance: 31% Fill: 0.87–0.96 (35) T_{FM} : -20.6 to -25°C (8) T_{LM} : -0.7 to -4.1°C (22) (1.2–6.6 eq. wt-%NaCl) $T_{\text{H}\rightarrow\text{L}}$: 101.6–201.8°C (35)	Abundance: 38% Fill: 0.82–0.97 (34) T_{FM} : -19.4 to -23.6°C (7) T_{LM} : -1.8 to -3.4°C (21) (3.1–6.2 eq. wt-%NaCl) $T_{\text{H}\rightarrow\text{L}}$: 86.6–260.3°C (33)	Abundance: 61% Fill: 0.71–0.99 (69) T_{FM} : -20.1 to -25.2°C (12) T_{LM} : -0.2 to -4.9°C (57) (0.4–7.7 eq. wt-%NaCl) $T_{\text{H}\rightarrow\text{L}}$: 140–296.7°C (69)

T_{FM} : first ice melting; T_{LM} : last ice melting; $T_{\text{H}\rightarrow\text{V}}$: homogenisation temperature to vapour; $T_{\text{H}\rightarrow\text{L}}$: homogenisation temperature to liquid; T_{D} : decrepitation temperature; F: degree of fill. Round brackets indicate the number of measurements. The degree of fill was measured by estimating the proportions of liquid and vapour at 25°C and comparing to published reference charts.⁶¹ The criteria of Ref. 27 was used to determine the genetic relationship between inclusions and their host quartz crystals.



a type 1 inclusion (vapour-rich) in DS4-06; b pseudosecondary trail of type 1 (vapour-rich) and type 2 inclusion (liquid-rich) in Shap granite; c trail of type 2 inclusions (liquid-rich) in DS6-06; d types 2 and 3 inclusions (liquid-rich) in DS6-06

6 Photomicrographs of fluid inclusion types

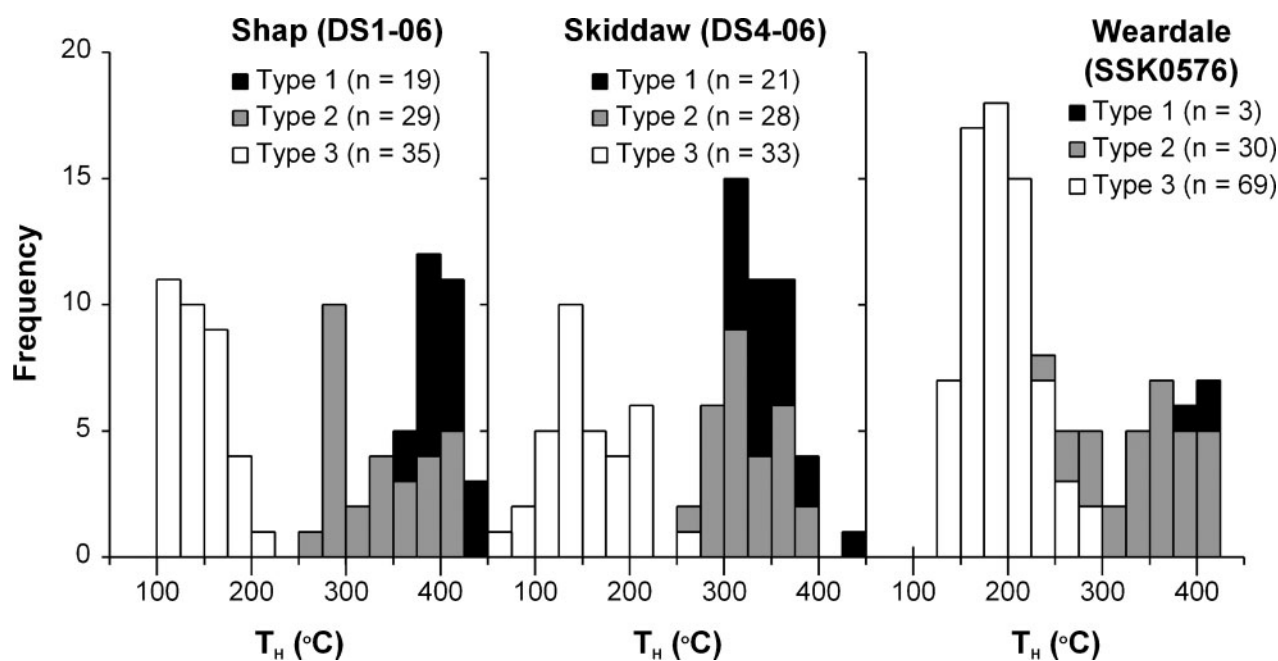
the non-aqueous phase, of CO₂, CH₄, N₂ and H₂S (Table 4 and Fig. 9). Types 1 and 2 inclusions in the vein quartz sample from the Shap granite have broadly similar and dominant abundances of CO₂ (about 90–99 mol.-%) with subordinate to trace amounts of N₂, CH₄ and trace H₂S. In contrast, types 1 and 2 inclusions hosted in vein quartz from the Skiddaw granite contain less CO₂ (about 41–85 mol.-%) coupled with higher abundances of CH₄ (about 3–15 mol.-%) and N₂ (11–44 mol.-%). Laser Raman microspectroscopy (LRM) of type 2 inclusions hosted in pegmatite vein quartz from

the Weardale granite did not detect the presence of CO₂, CH₄, N₂ or H₂S (Table 4).

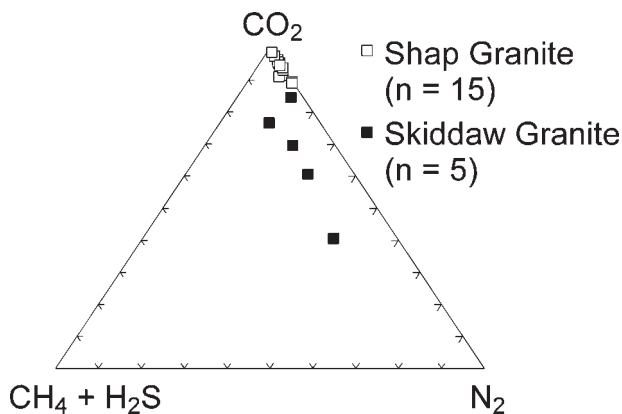
Discussion

Re–Os molybdenite and U–Pb zircon geochronology

Numerous studies have shown that the Re–Os systematics in molybdenite are robust, being unaffected by post-ore hydrothermal, metamorphic and magmatic activity.^{55,70} As a result, Re–Os molybdenite dates yield the timing of sulphide mineralisation. In mineral systems



7 T_H histograms for types 1–3 fluid inclusions in northern England



8 Bivariate plots of T_H and salinity (eq. wt-%NaCl) for types 1–3 fluid inclusions in northern England

genetically related to magmatism, Re–Os molybdenite ages are shown to be identical to U–Pb zircon ages for the progenitor intrusions.⁵⁷ This relationship suggests that Re–Os molybdenite ages, in granite-related systems, can provide a minimum age for magmatism.

The Shap granite

The Re–Os ages for disseminated (405.2 ± 1.8 Ma) and vein-hosted (405.5 ± 1.7 Ma) molybdenite are older and outside uncertainty of previous U–Pb, Rb–Sr and K–Ar age constraints^{51,71} (Fig. 2). The Re–Os ages suggest that magmatism and mineralisation occurred contemporaneously and ~ 8 m.y. earlier than previously considered (Fig. 2). The previous U–Pb, Rb–Sr and K–Ar age determinations likely reflect disturbance to the isotope systematics. The latter maybe accounted for by the alteration of matrix megacrysts, plagioclase and biotite to sericite and chlorite respectively, which is not observed in megacrysts within enclaves.¹⁰ Remarkably, given the employed analytical protocols at the time, the recalculated 1964 Re–Os molybdenite age³¹ is within uncertainty of the new Re–Os age (Fig. 2).

The new Re–Os molybdenite age (405 Ma) allows for the reinterpretation of a recent Rb–Sr dataset from a single plagioclase-rimmed K-feldspar megacryst within a mafic inclusion (enclave).¹³ The isochronous behaviour of the Rb–Sr data (405 ± 2 Ma), which requires the sample set to possess identical initial Sr isotope compositions, was not considered to reflect the timing of emplacement of the granite because the K–Ar (397 ± 7 Ma) and U–Pb (390 ± 6 Ma) determinations were considered reliable.¹³ Subsequently, the Rb–Sr data were used to show that the initial Sr isotope composition at 397 Ma of the K-feldspar (0.70762 and 0.70767) was more radiogenic than the plagioclase rim (0.70722 and 0.70739). This feature was considered to reflect that the K-feldspar formed in a more evolved granitic magma and interacted with a less evolved, mafic magma during the crystallisation of plagioclase, supporting magma mixing events.¹⁰ However, the initial Sr isotope compositions calculated at 405 Ma (Sr_{405Ma}) are almost identical (core inner: 0.70713, outer core: 0.70714, inner rim: 0.70713, outer rim: 0.70716), which match two of the three Sr_{405Ma} values for a K-feldspar megacryst in a basic enclave reported by Cox *et al.*¹⁰ As a result, the Sr_{405Ma} data demonstrate that there was only minor Sr isotopic heterogeneity in the magmas associated with the Shap granite and that the initial Sr composition is less

radiogenic (more juvenile) than previous determinations (cf. 0.70767).⁷¹ This re-interpretation of the Rb–Sr data further stresses that the absolute age and its uncertainty for granite emplacement is critical when applying Rb–Sr data to calculate initial isotopic compositions to evaluate magma sources and processes in ancient systems.^{14,63}

The Skiddaw granite

The emplacement age for the Skiddaw granite is given by a zircon concordia age of 398.8 ± 0.4 Ma (Fig. 5). This is in agreement with previous age constraints; however, it is considerably more precise: 398 ± 8 Ma for Rb–Sr K-feldspar from greisen-altered granite,⁵² and 399 ± 6 Ma for K–Ar biotite⁹ (Fig. 4). Molybdenite from a quartz–molybdenite–pyrite–chalcopyrite vein post-dating pervasive greisen alteration yields a Re–Os age of 392.3 ± 2.8 Ma (Table 1). This age is within uncertainty of the K–Ar ages for greisen muscovite (387 ± 4 Ma,^{52,59} and a Rb–Sr fluid inclusion age of 392 ± 5 Ma,⁶² determined from the analysis of early and late stage quartz veins associated with sulphide mineralisation. The Re–Os age also agrees within uncertainty of a mean K–Ar age (394 ± 8 Ma) interpreted to represent the final cooling of Skiddaw granite^{52,59} (Fig. 3). Whole-rock Rb–Sr analysis of altered granite yields a younger age (383 ± 4 Ma).

The disparity between U–Pb and Re–Os ages (398.8 ± 0.4 and 392.3 ± 2.8 Ma) suggests that the Skiddaw granite was emplaced several million years (~ 5 m.y.) before the sulphide mineralisation dated here. However, the Re–Os age does not negate the Skiddaw granite being the progenitor of the early stage (~ 0.5 m quartz Harding, Smith, Emerson veins) mineralisation of the Carrock W deposit.

Magmatic-hydrothermal systems are typically only sustained by a single intrusive event for a maximum of 800 k.y. and this duration drastically declines with an increase in permeability of the country rock.¹¹ However, minor chloritised magmatic biotite away from the mineralised zone (Sinen Gill) yield K–Ar ages (392 ± 8 Ma) that nominally agree with the timing of mineralisation may reflect the final cooling of the granite.⁵⁹ Therefore, either the Skiddaw granite is a more complex intrusion than exposed, representing multiple magmatic-hydrothermal pulses or a separate hydrothermal (non-magmatic) pulse occurred at ~ 392 m.y. as indicated by the Re–Os age for sulphide mineralisation (see below).

The Weardale granite

Molybdenite from a pre-aplite pegmatitic quartz vein yields a Re–Os age of 398.3 ± 1.6 Ma. The Re–Os age suggests that the emplacement of the Weardale granite and mineralisation occurred ~ 10 m.y. later than previously determined based on Rb–Sr wholerock analysis.³² The age for the aplite are based on determinations of one sample using the Sr initial composition (0.706 ± 0.002) from the regression of the granite wholerock data (390 ± 8 Ma).³² However, this age is based on one of two reported present day $^{87}Sr/^{86}Sr$ values (0.8656 ± 0.0028). The second $^{87}Sr/^{86}Sr$ value (0.8683 ± 0.0014), not discussed,³² yields an apparent age of 397 ± 8 Ma. Though the two ages for the aplite are within uncertainty, the latter is nominally in agreement with the Re–Os age and suggests a genetic

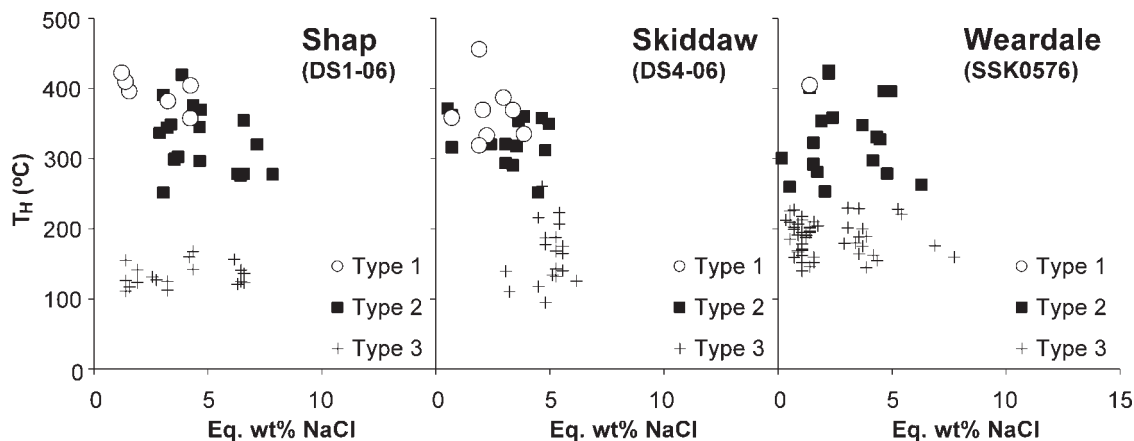
Table 4 Chemical composition of the non-aqueous phase of types 1 and 2 inclusions in the Shap, Skiddaw and Weardale granites, obtained from Raman microspectrometry: bulk fluid inclusion parameters calculated for inclusions on which full microthermometric analysis was obtained

Host granite	F.I. no.	F.I. type	Composition of the non-aqueous phase, mol.-%									Bulk fluid inclusion parameters							Molar volume †, cm ³ mol			
			CO ₂	CH ₄	N ₂	H ₂ S	Fill	T _{LM}	T _M C	T _H	XH ₂ O	XCO ₂	XCH ₄	XN ₂	XNaCl							
Shap (DS1-06)	1	1	99	0.3	<1	<0.1	0.24	5.9	383.4	(V)	0.24	5.9	383.4	(V)								
	2	1	95.5	<0.3	4	0.4	0.22	-1.1	381.5	(V)	0.22	-1.1	381.5	(V)								
	3	1	90	<0.3	10	n.d.																
	4	2	91.5	2.5	6	0.4	0.71	-2.5	344.6	(L)	0.71	-2.5	344.6	(L)	93.32	3.75	0.04	0.09	2.80		24.96	
	5	2	96	<0.3	4	n.d.	0.72	-1.3	329.4	(L)	0.72	-1.3	329.4	(L)								
	6	1	97	<0.3	3	n.d.	0.51	7	357.2	(V)	0.51	7	357.2	(V)								
	7	2	95.5	<0.3	4	0.1																
	8	2	96	<0.3	3.5	<0.1	0.65	-2.8	369.1	(L)	0.65	-2.8	369.1	(L)	93.31	3.79	0.01	0.06	2.83		27.25	
	9	2	89.5	0.5	10	n.d.	0.59	-3.1	375.7	(L)	0.59	-3.1	375.7	(L)	92.64	4.49	0.01	0.25	2.61		29.75	
	10	1	93.5	<0.3	6	n.d.																
	11	1	98	<0.3	1.8	<0.1	0.26	-1.4	398.7	(V)	0.26	-1.4	398.7	(V)								
	12	1	94	<0.3	5.5	<0.1	0.54	-1.3	404	(V)	0.54	-1.3	404	(V)	92.03	5.27	0.01	0.17	2.52		32.31	
	13	1	95	<0.3	4.5	0.3	0.54	-1.4	392	(V)	0.54	-1.4	392	(V)								
	14	1	99	<0.3	<1	0.1																
Skiddaw (DS4-06)	15	1	61	11	28	n.d.	0.36	-1	408*	(D)	0.36	-1	408*	(D)	89.12	6.14	0.79	2.00	1.96		46.41	
	16	2	41	15	44	n.d.	0.65	-1.7	230.4*	(D)	0.65	-1.7	230.4*	(D)								
	17	2	77	12	11	n.d.	0.59	-1.7	353.1	(L)	0.59	-1.7	353.1	(L)	91.25	5.63	0.52	0.47	2.12		30.16	
	18	1	70	10	20	n.d.	0.28	-1	386.7	(V)	0.28	-1	386.7	(V)	87.49	8.15	0.91	1.80	1.65		60.21	
Weardale (SSK0576)	19	2	85	3	12	n.d.	0.67	-1.4	357.3	(L)	0.67	-1.4	357.3	(L)	93.00	3.90	0.06	0.23	2.80		27.26	
	20	2	n.d.	n.d.	n.d.	n.d.	0.72	-0.6	390.8*	(D)	0.72	-0.6	390.8*	(D)	99.35				0.65		39.67	
	21	2	n.d.	n.d.	n.d.	n.d.	0.68		395*	(D)	0.68		395*	(D)								
	22	2	n.d.	n.d.	n.d.	n.d.	0.55	-1	387	(D)	0.55	-1	387	(D)	98.92				1.08		37.45	

Composition of the non-aqueous phase obtained from Raman microprobe spectrometry. F.I.=fluid inclusion; n.d.=not detected. T_{LM}=last ice melting temperature (°C); T_MC=Clathrate melting temperature (°C); T_H homogenisation temperature (°C).

*Temperature of decrepitation.

†Bulk fluid inclusion parameters calculated using the ICE-CLATHRATE program.



9 CO_2 v. $\text{CH}_4 + \text{H}_2\text{S}$ v. N_2 triplot for types 1 and 2 inclusions in the Shap and Skiddaw granites

relationship with the Weardale magma. In addition, though within uncertainty, the reporting of two present day $^{87}\text{Sr}/^{86}\text{Sr}$ values (DH7, 11)³² may suggest some uncertainty in the Sr data reported by Holland and Lambert³² and subsequently the determined Rb–Sr age for the Weardale granite.

Fluids (types 1–3) in the Mo-bearing veins from Shap, Skiddaw and Weardale granites

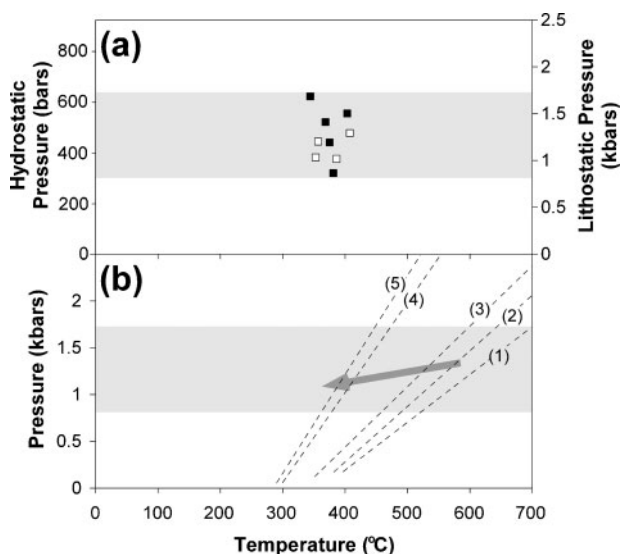
The Mo-bearing veins from each of the three granites contain a similar range of fluid inclusion types, i.e. types 1–3. Microthermometry of all three types indicates similar fluid salinities that range between ~0 and ~8 eq. wt-%NaCl. T_{H} histograms (Fig. 7) for types 1–

3 fluid inclusions indicate a progressive decrease in homogenisation temperatures from type 1 (~450°C) through to type 3 (~150°C). Bivariate plots of T_{H} versus salinity, however, show no obvious correlations between salinity and homogenisation temperatures (Fig. 8). Significant differences in fluid compositions between the three veins are revealed, however, by combining the LRM data with the microthermometric data.

Vapour-rich type 1 and liquid-rich type 2 inclusions in the Shap and Skiddaw veins are found in the same FIA and T_{H} measurements from coexisting types 1 and 2 inclusions are identical ($\pm 10^\circ\text{C}$). This suggests that types 1 and 2 inclusions were trapped from immiscible fluids (i.e. boiling) during vein emplacement and Mo mineralisation.

The non-aqueous phases in types 1 and 2 inclusions from the Shap vein are dominated by CO_2 (89.5–99 mol.-%) with low abundances of N_2 (<10 mol.-%) and CH_4 (<1 mol.-%; Table 3 and Fig. 9). The presence of CO_2 combined with the low levels of N_2 in these fluids (mean=4.5 mol.-%) suggests that these fluids are magmatic in origin.³³ A predominant magmatic origin for mineralising fluids is also supported by $\delta^{34}\text{S}$ values for sulphide minerals from –1 to +5‰,³⁶ consistent with I-type magmas.³⁷

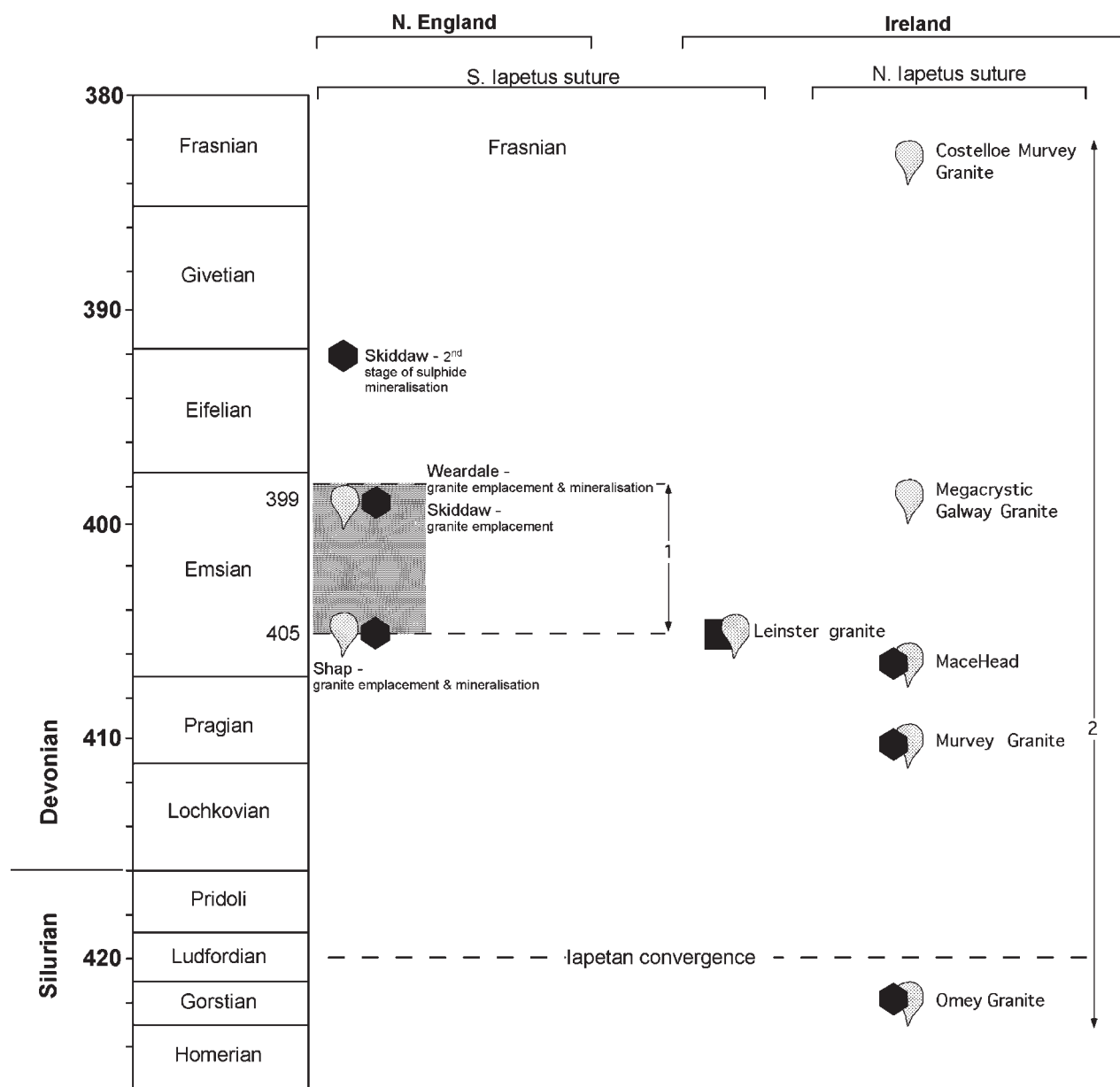
The types 1 and 2 inclusions in the Skiddaw vein contain relatively high abundances of CH_4 (up to 15 mol.-%) and N_2 (up to 44 mol.-%) in comparison to the Shap vein (Table 3 and Fig. 8). The high N_2 content in these fluids indicates an influx of metamorphic fluids.³³ Nitrogen enrichment is also a feature in the greisen altered Skiddaw Granite and this together with the recorded decrease in countryrock N_2 from >800 ppm (2.5 km away from the contact) to <410 ppm ~0.5 km from the contact⁵ is further evidence of countryrock involvement in fluid compositions. The latter may also be suggested by the sub-ppm Re concentrations [0.75 ppm (0.47 ppm ^{187}Re), Table 1] in molybdenite from the Carrock deposit (DS4-06). For example, low Re-bearing (<5 ppm) molybdenite associated with W and Sn mineralisation is common to metamorphic-related environments and ore-fluids.⁶⁰ However, molybdenite associated with magmatic-related mineral systems typically has high Re concentrations (tens to thousands of ppm) (cf. Refs. 40 and 56, and references therein,^{4,60} and references therein and the Shap and Weardale granites of this study).



a trapping conditions of types 1 and 2 inclusions in samples DS1-06 (Shap) and DS4-06 (Skiddaw); shaded area represents estimated trapping pressures; trapping conditions calculated according to the equation of state of Ref. 18; b isochores constructed from individual type 2 FIA in sample SSK0576 (Weardale)

10 Pressure–temperature space showing trapping temperatures and pressures for types 1 and 2 inclusions: arrow represents isobaric cooling during fluid evolution; FIA (1): $T_{\text{H}}=395^\circ\text{C}$, salinity=4.65 eq. wt-%NaCl; FIA (2): $T_{\text{H}}=380^\circ\text{C}$, salinity=4.96 eq. wt-%NaCl; FIA (3): $T_{\text{H}}=350^\circ\text{C}$, salinity=2 eq. wt-%NaCl; FIA (4): $T_{\text{H}}=300^\circ\text{C}$, salinity=0.18 eq. wt-%NaCl; FIA (5): $T_{\text{H}}=290^\circ\text{C}$, salinity=1.57 eq. wt-%NaCl

Frasnian



11 Diagram showing the timing relationships between magmatism (○) and mineralisation (◆=molybdenite, ■=sulphide) across the northern England and Irish sector of the Appalachian-Caledonian orogen: timing of the main Acadian deformation front is pre-405 Ma, but was episodic throughout the Emsian; magmatism in the north of the Iapetus suture was initiated when orogen parallel structures (e.g. Great Glen and Southern Upland Faults) were active;⁶⁸ time-scale after Gradstein *et al.*²⁹

Type 1 inclusions are very rare in the Weardale granite's Mo-bearing quartz pegmatite vein. The type 2 inclusions invariably occur in annealed fractures. Furthermore, the lack of obvious clathration in types 1 and 2 inclusions coupled with the LRM data for type 2 inclusion fluids indicates significant differences in their fluid composition to those recorded in the Shap and Skiddaw veins. However, the types 1 and 2 inclusions are found in pseudosecondary trails and represent fluids

present during the crystallisation of this pegmatite. As type 1 inclusions make up only ~3% of the total fluid inclusion population, fluid boiling in the Weardale granite was relatively minor and this may be related to the lack of gaseous species within mineralising fluids (as indicated by LRM). Based on the petrographic setting of type 2 inclusions, they are interpreted as representing late-stage magmatic fluids containing little or no non-aqueous species.

The salinities of type 3 inclusion fluids from all three veins are similar to the salinities of types 1 and 2 inclusion fluids. However, their homogenisation temperatures are relatively low (Fig. 8). Furthermore, type 3 inclusions are confined to annealed fractures reflecting lower temperature fluid influxes that may be meteoric in origin and similar to meteoric fluids recorded in other late-Caledonian granites.^{12,24,49}

P–T modelling of fluid trapping conditions

The presence of vapour-rich (type 1) and liquid-rich (type 2) inclusions in the Shap and Skiddaw veins may reflect fluid boiling. This may also be true in the case of the Weardale vein although type 1 inclusions are rare. If it is assumed that boiling occurred in the Shap and Skiddaw veins, then T_H equates to the true trapping temperature T_T of the fluids. In addition, trapping pressures of inclusions can be calculated using the volume and bulk composition of fluids (Table 3).

Trapping temperatures and pressures of types 1 and 2 inclusions in the Shap and Skiddaw veins were calculated¹⁸ and are plotted in Fig. 10a. Calculated trapping pressures (assuming a hydrostatic pressure gradient of 98.1 bar km^{-1} ;⁶¹ for the Shap and Skiddaw, veins' inclusions are between 300 and 620 bars (3–6.3 km) and 375–475 bars (3.8–4.9 km) respectively. These emplacement depths are consistent with fluid inclusion data from wolframite-bearing quartz veins in the Skiddaw granite, which indicates that mineralisation occurred at depths $>1.4 \text{ km}$.³

The rarity of vapour-rich type 1 inclusions in the Weardale vein is considered to reflect the absence of boiling and therefore, a pressure correction is required to determine the fluid trapping conditions. In Fig. 10b, isochores were constructed for individual type 2 FIA using the program FLUIDS.² Assuming that the Weardale granite was emplaced at a similar crustal level to the Shap and Skiddaw granites (3–6.3 km), then type 2 inclusions were trapped at lithostatic pressures of 1–1.7 kbars and were trapped at progressively lower temperatures (about 650–350°C) during isobaric cooling.

Implications

New Re–Os molybdenite ages indicate that emplacement and mineralisation of the Shap, Skiddaw and Weardale granites occurred during the upper Early Devonian (Emsian) and not during the lower Middle Devonian (Eifelian) (Fig. 11). However, mineralisation associated with the Carrock deposit (Skiddaw granite), in part, occurred during the Eifelian (Fig. 11). Additionally, the Shap granite has long been recognised to post-date deformation (main cleavage development) as shown by contact metamorphic minerals, at several localities, occurring in random orientation across the cleavage of the country rocks.⁷ In contrast, in the Skiddaw, aureole andalusite both pre- and post-dates the main cleavage.⁶⁴ Previous attempts to constrain the timing of the Acadian tectonometamorphic events have been less definitive in northern England and Wales because of: the range in Rb–Sr, K–Ar and Ar–Ar ages; the behaviour of the isotopic systems; and the interpretation of the ages.^{17,21,22,43} Broadly, K–Ar and Ar–Ar ages suggest apparent contemporaneous deformation at 400 Ma.^{17,21,22,43,65} The Re–Os and U–Pb ages of this study establish the non-synchronous development of cleavage of the Acadian deformation front in the Lake

District occurred before $\sim 405 \text{ Ma}$ (emplacement of the Shap granite) and continued episodically throughout the Emsian ($\sim 398 \text{ Ma}$, Skiddaw granite; Fig. 11).

The broad timing and fluid characteristics of the granite emplacement and Mo-mineralisation in the Shap, Skiddaw and Weardale granites coincide with that of the Irish sector of the C-AO (Fig. 11). For example, combined fluid inclusion data and U–Pb and Re–Os geochronology have shown that granite-related molybdenite mineralisation in the Connemara region was accompanied by aqueous-carbonic fluids in the Omev Granite at $\sim 422 \text{ Ma}$ and later, in the western sector of the Galway Batholith at $\sim 410 \text{ Ma}$ (Murvey) and $\sim 407 \text{ Ma}$ (Mace Head).^{25,28,49} Further magmatism and W–Sn-sulphide mineralisation is associated with the $\sim 405 \text{ Ma}$ Leinster granite, SE Ireland.^{49,50}

The diachronous granite emplacement between northern England and Irish sector of the C-AO during the Acadian phase may relate to the oblique 'soft' collision plate convergence of eastern Avalonia with Laurentia^{15,66} associated with sinistral transtension during the Emsian.^{15,65} For example, in the Connemara region, granite-related Mo-mineralisation systems were initiated when orogen parallel structures (e.g. Great Glen and Southern Upland Faults) were active.¹⁵ They continued as part of the stitching Galway Batholith's evolution (410–380 Ma) when these major lineaments had ceased to be active.²³ In contrast, south of the Iapetus suture granite systems of northwest England and southeast Ireland were emplaced following the main Acadian deformation front.⁶⁵

Conclusions

Molybdenite Re–Os and U–Pb zircon geochronology and fluid inclusion data presented in this study define the timing and fluid characteristics associated with sulphide mineralisation in the Lake District, and the nature and relationship between mineralisation and magmatism.

The Re–Os ages for mineralisation in the Shap Granite range are $405.2 \pm 1.8 \text{ Ma}$ (disseminated molybdenite) and $405.5 \pm 1.7 \text{ Ma}$ (vein-hosted molybdenite). These ages are older than previously published U–Pb, Rb–Sr and K–Ar age constraints and indicate that mineralisation and magmatism occurred during the Emsian. Fluid inclusion analysis shows that mineralisation in the Shap Granite is associated with the boiling of CO_2 -rich late magmatic fluids between 300 and 450°C, at hydrostatic pressures of between 440 and 620 bars.

Zircon U–Pb geochronology yields an emplacement age of the Skiddaw granite at $398.8 \pm 0.4 \text{ Ma}$. Molybdenite mineralisation that post-dates the main W mineralisation yields a Re–Os age of $392.3 \pm 2.8 \text{ Ma}$. The non-aqueous compositions of mineralising fluids and Re concentrations in molybdenite are consistent with a non-magmatic source for sulphide mineralisation, in contrast to earlier W mineralisation.^{3,59} Instead, mineralising fluids extensively interacted with the surrounding country rocks, becoming enriched in isotopically heavy sulphur, N_2 and CH_4 . The elevated non-aqueous component of these fluids (up to 12.5 wt-%) facilitated boiling between 275 and 400°C and at hydrostatic pressures of 375–475 bars.

Mineralisation in the Weardale granite is hosted in a molybdenite bearing quartz pegmatite vein, and yields a Re–Os age of $398.3 \pm 1.6 \text{ Ma}$. No evidence for fluid

boiling has been recorded, and mineralising fluids represent late stage magmatic fluids trapped at high temperatures (476–577°C) and at lithostatic pressures of 1–1.7 kbars.

The new U–Pb and Re–Os ages reported in this study place constraints on the timing of main Acadian deformation in the Lake District, the eastern Avalonia sector of the C-AO. Acadian deformation was episodic and diachronous beginning before the emplacement of the Shap Granite at ~405 Ma, and continued episodically throughout the Emsian (~398 Ma, emplacement of the Skiddaw granite). This study confirms the notion that the timing of magmatism in northern England also coincides with that of the Irish sector of Avalonia.

Acknowledgements

D. Selby would like to acknowledge the Nuffield Bursary placement for secondary school students (SETPOINT North East Centre for Lifelong Learning) through which the initial stages of this study were undertaken by S. Baggaley. F. McEvoy and M. Howe of the British Geological Survey are thanked for providing the molybdenite sample from the Weardale granite. T. Lhlomme, at CREGU, Nancy, France, is thanked for conducting the Raman microspectroscopy analysis. N. Blamey, NUIG, is acknowledged for discussions on fluid evolution. J. LaFace and C. Thomson are thanked for their assistance in the field and for sample preparation. J. Evans is thanked for giving access to the previously collected Skiddaw granite samples, N. Boulton and A. Sumner are thanked for technical assistance at NIGL. The U–Pb ID-TIMS portion of this study was funded by the BGS-NIGL programme (continental arc volcanism, fluid evolution and metallogenesis in the Lake District, project no. 40200). M. Bussell and an anonymous Applied Earth Science reviewer are thanked for their comments.

References

- R. J. Bakker: 'Clathrates: computer programs to calculate fluid inclusion V–X properties using clathrate melting temperatures', *Comput. Geosci.*, 1997, **23**, 1–18.
- R. J. Bakker: 'Package FLUIDS 1. Computer programs for analysis of fluid inclusion data and for modeling bulk fluid properties', *Chem. Geol.*, 2003, **194**, 3–23.
- T. K. Ball, N. J. Fortey and T. J. Shepherd: 'Mineralisation at the Carrock Fell tungsten mine, N. England: paragenetic, fluid inclusion and geochemical study', *Miner. Depos.*, 1985, **20**, 57–65.
- F. Barra, J. Ruiz, R. Mathur and S. Titley: 'A Re–Os study of sulfide minerals from the Bagdad porphyry Cu–Mo deposit, northern Arizona, USA', *Miner. Depos.*, 2003, **38**, 585–596.
- G. E. Bebout, D. C. Cooper, A. D. Bradley and S. J. Sadofsky: 'Nitrogen-isotope record of fluid-rock interactions in the Skiddaw aureole and granite, English Lake District', *Am. Mineral.*, 1999, **84**, 1495–1505.
- R. J. Bodnar: 'Revised equation and table for determining the freezing point depression of H₂O–NaCl solutions', *Geochim. Cosmochim. Acta*, 1993, **57**, 683–684.
- C. A. Boulter and N. J. Soper: 'Structural relationships of the Shap granite', *Proc. Yorkshire Geol. Soc.*, 1973, **39**, 365–369.
- P. E. Brown, J. A. Miller and K. L. Grastly: 'Isotopic ages of the late Caledonian granitic intrusions in the British Isles', *Proc. Yorkshire Geol. Soc.*, 1968, **34**, 331–342.
- P. E. Brown, J. A. Miller and N. J. Soper: 'Age of the principal intrusions of the Lake District', *Proc. Yorkshire Geol. Soc.*, 1964, **34**, 331–342.
- R. A. Cox, T. J. Dempster, B. R. Bell and G. Rogers: 'Crystallization of the Shap Granite: evidence from zoned K-feldspar megacrysts', *J. Geol. Soc. (Lond.)*, 1996, **153**, 625–635.

- L. M. Cathles, A. H. J. Erendi and T. Barrie: 'How long can a hydrothermal system be sustained by a single intrusive event?', *Econ. Geol.*, 1997, **92**, 766–771.
- J. Conliffe and M. Feely: 'Microthermometric characteristics of fluids associated with granite and greisen quartz, and vein quartz and beryl from the Rosses Granite Complex, Donegal, NW Ireland', *J. Geochem. Explor.*, 2006, **89**, 73–77.
- J. P. Davidson, B. Charlier, J. M. Hora and R. Perlroth: 'Mineral isochrons and isotopic fingerprinting: pitfalls and promises', *Geology*, 2005, **33**, 29–32.
- J. P. Davidson, L. Font, B. L. A. Charlier and F. J. Tepley: 'Mineral-scale Sr isotope variation in plutonic rocks – a tool for unraveling the evolution of magma systems', *Trans. R. Soc. (Edinb.)*, to be published.
- J. F. Dewey and R. A. Strachan: 'Changing Silurian-Devonian relative plate motion in the Caledonides: sinistral transpression to sinistral transtension', *J. Geol. Soc. (Lond.)*, 2003, **160**, 219–229.
- M. H. Dobson and S. Moorbath: 'Isotopic ages of the Weardale granite', *Nature*, 1961, **190**, 899.
- H. Dong, C. M. Hall, A. N. Halliday, D. R. Peacor, R. J. Merriman and B. Roberts: '⁴⁰Ar/³⁹Ar illite dating of Late Caledonian (Acadian) metamorphism and cooling of K-bentonites and slates from the Welsh Basin, UK', *Earth Planet. Sci. Lett.*, 1997, **150**, 337–351.
- Z. Duan, N. Moller and J. H. Weare: 'A general equation of state for supercritical fluid mixtures and molecular dynamics simulation of mixture PVTX properties', *Geochim. Cosmochim. Acta*, 1996, **60**, 1209–1216.
- J. Dubessy, B. Poty and C. Ramboz: 'Advances in C–O–H–N–S fluid geochemistry based on micro-Raman spectrometric analysis of fluid inclusions', *Eur. J. Mineral.*, 1989, **1**, 517–537.
- K. C. Dunham: 'Geology of the Northern Pennine Orefield', *Br. Geol. Surv.*, 1990, **1**, 299.
- J. A. Evans: 'Dating the transition of smectite to illite in Palaeozoic mudrocks using the Rb–Sr whole-rock technique', *J. Geol. Soc. (Lond.)*, 1996, **153**, 101–108.
- J. A. Evans, I. L. Millar and S. R. Noble: 'Hydration during uplift is recorded by reset Rb–Sr whole-rock ages', *J. Geol. Soc. (Lond.)*, 1995, **152**, 209–212.
- M. Feely, D. Coleman, S. Baxter and B. Miller: 'U–Pb zircon geochronology of the Galway Granite, Connemara, Ireland: implications for the timing of late Caledonian tectonic and magmatic events and for correlations with Acadian plutonism in New England', *Atlant. Geol.*, 2003, **39**, 175–184.
- M. Feely, J. Conliffe, K. Faure and S. E. Power: 'Fluid inclusion trails in granite quartz: evidence for aqueous fluid infiltration in the Oughterard Granite, Eastern Connemara', *Irish J. Earth Sci.*, 2006, **24**, 1–11.
- M. Feely, D. Selby, J. Conliffe and M. Judge: 'Re–Os geochronology and fluid inclusion microthermometry of molybdenite mineralisation in the late-Caledonian Omev granite, western Ireland', *Trans. Inst. Min. Metall. B, Appl. Earth Sci.*, 2007, **116B**, 143–149.
- F. J. Fitch and J. A. Miller: 'Age of the Weardale granite', *Nature*, 1965, **208**, 743–745.
- R. H. Goldstein: 'Re-equilibrium of fluid inclusions', *Mineral. Assoc. Can. Short Course Ser.*, 2003, 9–53.
- V. Gallagher, M. Feely, H. Hogelsberger, G. R. T. Jenkin and A. E. Fallick: 'Geological, fluid inclusion and stable isotope studies of Mo mineralisation, Galway Granite, Ireland', *Miner. Depos.*, 1992, **27**, 314–325.
- F. M. Gradstein, J. G. Ogg, A. G. Smith, F. P. Agterberg, W. Bleeker, R. A. Cooper, V. Davydov, P. Gibbard, L. A. Hinnov, M. R. House, J. Lourens, H. P. Luterbacher, J. McArthur, M. J. Melchin, L. J. Robb, J. Shergold, M. Villeneuve, B. R. Wardlaw, J. Ali, H. Brinkhuis, F. J. Hilgen, J. Hooker, R. J. Howarth, A. H. Knoll, J. Lasker, S. Monechi, J. Powell, K. A. Plumb, I. Raffi, U. Rohl, A. Sanfilippo, B. Schmitz, N. J. Shackelton, G. A. Shields, H. Strauss, J. van Dam, J. Veizer, T. Vav Kolfschoten and D. Wilson: 'A geologic time scale 2004', 2004, Cambridge, Cambridge University Press.
- J. W. Hedenquist and R. W. Henley: 'The importance of CO₂ on freezing point measurements of fluid inclusions; evidence from active geothermal systems and implications for epithermal ore deposition', *Econ. Geol.*, 1985, **80**, 1379–1406.
- W. Herr, R. Wolfle, P. Eberhardt and E. Kopp: 'Development and recent applications of the Re/Os dating method', in 'Radioactive dating and methods of low-level counting', 499–508; 1964, Vienna, IAEA.
- J. G. Holland and R. Lambert: 'Weardale granite', *Trans. Nat. Hist. Soc. Northumberland Durham Newcastle*, 1970, **41**, 103–118.

33. T. A. Huff and P. I. Nabelek: 'Production of carbonic fluids during metamorphism of graphitic pelites in a collisional orogen – an assessment from fluid inclusions', *Geochim. Cosmochim. Acta*, 2007, **71**, 4997–5015.
34. R. A. Hughes, J. A. Evans, S. R. Noble and C. C. Rundle: 'U–Pb chronology of the Ennerdale and Eskdale intrusions supports sub-volcanic relationships with the Borrowdale Volcanic Group (Ordovician, English Lake District)', *J. Geol. Soc. (Lond.)*, 1996, **153**, 33–38.
35. T. E. Krogh: 'Improved accuracy of U–Pb zircon ages by the creation of more concordant systems using an air abrasion technique', *Geochim. Cosmochim. Acta*, 1982, **46**, 637–649.
36. D. Lowry, A. J. Boyce, R. A. D. Pattrick, A. E. Fallick and C. J. Stanley: 'A sulphur isotopic investigation of the potential sulphur sources for lower Palaeozoic-hosted vein mineralization in the English Lake District', *J. Geol. Soc. (Lond.)*, 1991, **148**, 993–1004.
37. R. Laouar, A. J. Boyce, A. E. Fallick and B. E. Leake: 'A sulphur isotope study on selected Caledonian granites of Britain and Ireland', *Geol. J.*, 1990, **25**, 359–369.
38. K. R. Ludwig: 'Calculation of uncertainties of U–Pb isotope data', *Earth Planet. Sci. Lett.*, 1980, **46**, 212–220.
39. K. Ludwig: 'Isoplot/Ex, version 3: a geochronological toolkit for Microsoft Excel'; 2003, Berkeley, CA, Geochronology Center Berkeley.
40. T. E. McCandless, J. Ruiz and A. R. Campbell: 'Rhenium behavior in molybdenite in hypogene and near-surface environments: implications for Re–Os geochronometry', *Geochim. Cosmochim. Acta*, 1993, **57**, 889–905.
41. R. Markey, H. Stein and J. Morgan: 'Highly precise Re–Os dating for molybdenite using alkaline fusion and NTIMS', *Talanta*, 1998, **45**, 935–946.
42. J. M. Mattinson: 'Zircon U–Pb chemical abrasion ("CA-TIMS") method: combined annealing and multi-step partial dissolution analysis for improved precision and accuracy of zircon ages', *Chem. Geol.*, 2005, **220**, 47–66.
43. R. J. Merriman, D. C. Rex, N. J. Soper and D. R. Peacor: 'The age of Acadian cleavage in northern England, UK: K–Ar and TEM analysis of a Silurian metabentonite', *Proc. Yorkshire Geol. Soc.*, 1995, **50**, 255–265.
44. D. Millward: 'Early Palaeozoic magmatism in the English Lake District', *Proc. Yorkshire Geol. Soc.*, 2002, **54**, 65–93.
45. D. Millward and J. A. Evans: 'U–Pb chronology and duration of late Ordovician magmatism in the English Lake District', *J. Geol. Soc. (Lond.)*, 2003, **160**, 773–781.
46. R. Mundil, K. R. Ludwig, I. Metcalfe and P. R. Renne: 'Age and timing of the Permian mass extinctions: U/Pb dating of closed-system zircons', *Science*, 2004, **305**, 1760–1763.
47. S. R. Noble, R. D. Tucker and T. C. Pharaoh: 'Lower Paleozoic and Precambrian igneous rocks from eastern England and their bearing on late Ordovician closure of the Tornquist sea: constraints from U–Pb and Nd isotopes', *Geol. Mag.*, 1993, **130**, 835–846.
48. S. Noble, J. Schweiters, D. J. Condon, Q. G. Crowley, N. Quaas and R. R. Parrish: 'TIMS characterization of new generation of secondary electron multiplier', *EOS Trans. AGU*, 2006, **87**, (52).
49. C. O'Reilly, G. R. T. Jenkin, M. Feely, D. H. M. Alderton and A. E. Fallick: 'A fluid inclusion and stable isotope study of 200 Ma of fluid evolution in the Galway Granite, Connemara, Ireland', *Contrib. Mineral. Petrol.*, 1997, **129**, 120–142.
50. P. J. O'Connor, M. Aftalion and P. S. Kennan: 'Isotopic U–Pb ages of zircon and monazite from the Leinster Granite, southeast Ireland', *Geol. Mag.*, 1989, **126**, 725–728.
51. R. T. Pidgeon and M. Aftalion: 'Cogenetic and inherited zircon U–Pb systems in granites: Palaeozoic granites of Scotland and England', in 'Crustal evolution in northwestern Britain and adjacent areas', (ed. D. R. Bowes and B. E. Leake), *Geol. J. Spec. Issue*, **10**, 1978, 183–220.
52. C. C. Rundle: 'The chronology of igneous intrusion in the English Lake District', PhD thesis, University of London, London, 1982.
53. D. Selby and R. A. Creaser: 'Macroscale NTIMS and microscale LA–MC–ICP–MS Re–Os isotopic analysis of molybdenite: testing spatial restriction for reliable Re–Os age determinations, and implications for the decoupling of Re and Os within molybdenite', *Geochim. Cosmochim. Acta*, 2004, **68**, 3897–3908.
54. D. Selby and R. A. Creaser: 'Re–Os geochronology and systematics in molybdenite from the Endako porphyry molybdenum deposit, British Columbia, Canada', *Econ. Geol.*, 2001, **96**, 197–204.
55. D. Selby, R. A. Creaser, C. J. R. Hart, C. S. Rombach, J. F. H. Thompson, M. T. Smith, A. A. Bakke and R. J. Goldfarb: 'Absolute timing of sulfide and gold mineralization: A comparison of Re–Os molybdenite and Ar–Ar mica methods from the Tintina Gold Belt, Alaska', *Geology*, 2002, **30**, 791–794.
56. D. Selby, R. A. Creaser, L. M. Heaman and C. J. R. Hart: 'Re–Os and U–Pb geochronology of the Clear Creek, Dublin Gulch, and Mactung deposits, Tombstone Gold belt, Yukon, Canada: absolute timing relationships between plutonism and mineralization', *Can. J. Earth Sci.*, 2003, **40**, 1839–1852.
57. D. Selby, R. A. Creaser, H. J. Stein, R. J. Markey and J. L. Hannah: 'Assessment of the ^{187}Re decay constant accuracy and precision: cross calibration of the ^{187}Re – ^{187}Os molybdenite and U–Pb zircon chronometers', *Geochim. Cosmochim. Acta*, 2007, **71**, 1999–2013.
58. M. I. Smoliar, R. J. Walker and J. W. Morgan: 'Re–Os isotope constraints on the age of Group IIA, IIIA, IVA, and IVB iron meteorites', *Science*, 1996, **271**, 1099–1102.
59. T. J. Shepherd, R. D. Beckinsale, C. C. Rundle and J. Durham: 'Genesis of Carrock Fell tungsten deposits, Cumbria: fluid inclusion and isotopic study', *Trans. Inst. Min. Metall. B, Appl. Earth Sci.*, 1976, **85B**, 63–73.
60. T. J. Shepherd and P. Waters: 'Fluid inclusion gas studies, Carrock Fell tungsten deposit, England: implications for regional exploration', *Miner. Depos.*, 1984, **19**, 304–314.
61. T. J. Shepherd, A. H. Rankin and D. H. M. Alderton: 'A practical guide to fluid inclusions'; 1985, London, Blackie.
62. T. J. Shepherd and D. P. F. Darbyshire: 'Fluid inclusion Rb–Sr isochrons for dating mineral deposits', *Nature*, 1981, **290**, 578–579.
63. W. Siebel, E. Reitter, T. Wenzel and U. Blaha: 'Sr isotope systematics of K-feldspars in plutonic rocks revealed by the Rb–Sr microdrilling technique', *Chem. Geol.*, 2005, **222**, 183–199.
64. N. J. Soper and D. E. Roberts: 'Age of cleavage in the Skiddaw slates in relation to the Skiddaw aureole', *Geol. Mag.*, 1971, **108**, 293–302.
65. N. J. Soper, B. C. Webb and N. H. Woodcock: 'Late Caledonian (Acadian) transpression in northwest England: timing, geometry and geotectonic significance', *Proc. Yorkshire Geol. Soc.*, 1987, **46**, 175–192.
66. N. J. Soper, R. A. Strachan, R. E. Holdsworth, R. A. Gayer and R. O. Greiling: 'Sinistral transpression and the silurian closure of Iapetus', *J. Geol. Soc. (Lond.)*, 1992, **149**, 871–880.
67. J. S. Stacey and J. D. Kramers: 'Approximation of terrestrial lead isotope evolution by two-stage model', *Earth Planet. Sci. Lett.*, 1975, **26**, 207–221.
68. H. J. Stein: 'Low-rhenium molybdenite by metamorphism in northern Sweden: Recognition, genesis, and global implications', *Lithos*, 2006, **87**, 328–346.
69. H. J. Stein, R. J. Markey and J. W. Morgan: 'Highly precise and accurate Re–Os ages for molybdenite from the east Qinling molybdenum, Shaanxi province, China', *Econ. Geol.*, 1997, **92**, 827–835.
70. H. J. Stein, J. W. Morgan, R. J. Markey and J. L. Hannah: 'An introduction to Re–Os: what's in it for the mineral industry?', *SEG Newslett.*, 1998, **32**, 8–15.
71. A. J. Wadge, N. H. Gale and R. D. Beckinsale: 'A Rb–Sr isochron for the Shap Granite', *Proc. Yorkshire Geol. Soc.*, 1978, **42**, 297–305.

Biography

David Selby graduated with a BSc degree (Hons) in Geology from University of Southampton, UK, in 1994, and subsequently gained a PhD degree from University of Alberta, Canada, on the fluid geochemistry of porphyry Cu–Mo–Au systems. Following post-doctoral work at Alberta on several aspects of Re–Os geochronology (molybdenite and other sulphides, black shales and oil), he became a lecturer at Durham University, UK, in 2005.

James Conliffe graduated with a BSc degree (2002) in Earth Science from NUIG. He recently completed a PhD degree on fluid inclusions in Irish granites (2007).

Quentin Crowley graduated with a BSc degree (Hons) in Geology in 1993 and completed a PhD degree in 1997 in aspects of field, geochemical and tectonic evolution of the Galway Granite Batholith (both from the National University of Ireland Galway, NUIG). Following an NUIG lectureship, he took up a post-doctoral research position at Keele University, England, as part of a European-wide research network investigating the

assembly of Central Europe in the Palaeozoic (1998–2002). Subsequent to this, he became an Associate Lecturer with the Open University (2002) and in the same year, was appointed manager of the U–Th–Pb geochronology laboratory at the NERC Isotope Geosciences Laboratory in Nottingham, England.

Martin Feely graduated with a BSc degree in Geology from the National University of Ireland Galway (NUIG) in 1973, an MSc degree (1978) in Geology

from University College Dublin and a PhD degree (1982) from NUIG. Following postdoctoral work at NUIG on radioelements in Irish granites, he joined the staff of NUIG's Geology Department in 1985. He is currently a senior lecturer at NUIG. He was also adjunct Associate Professor of Earth Sciences at Boston University (1997–2005) and is currently adjunct Professor of Geological and Environmental Sciences at James Madison University, VA, USA. He is manager of the Geofluids Research Group at NUIG.